

FIG. 1. X-ray star camera.

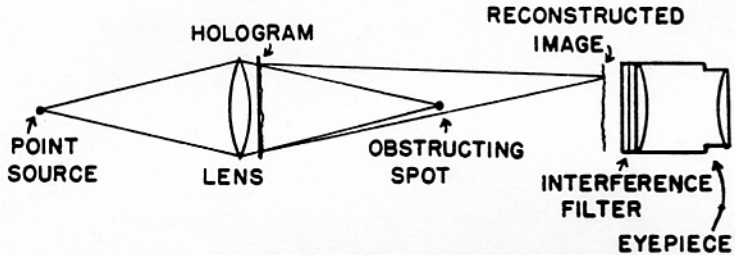


FIG. 3. Hologram reconstruction.

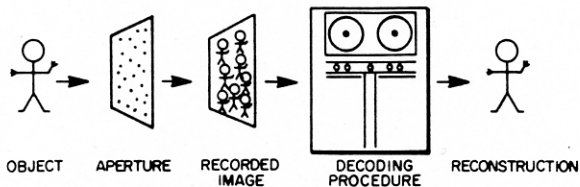
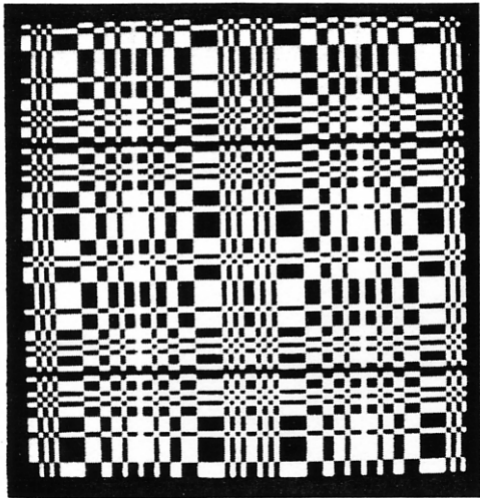
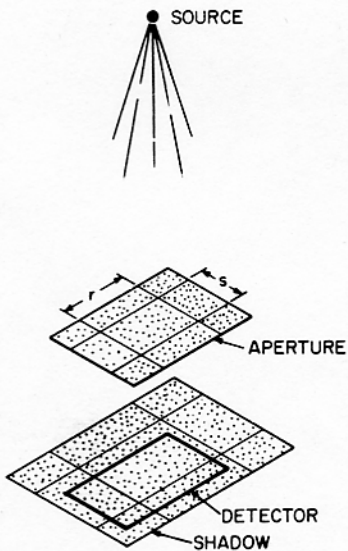


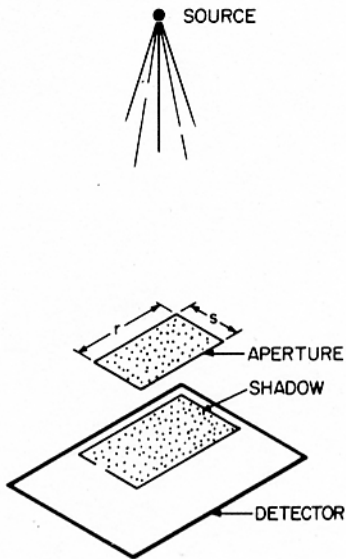
Fig. 1. The basic steps involved in coded aperture imaging are shown above. In an attempt to obtain a higher SNR, a multiple-pinhole aperture is used to form many overlapping images of the object. The resulting recorded picture must be decoded, using either a digital or optical method. The resulting reconstruction is of higher quality than that obtained by using a simple pinhole.





GEOMETRY No. 1

Fig. 3. This arrangement for a coded aperture imaging system employs a $2r$ by $2s$ aperture composed of a mosaic of basic r by s patterns. Emitting points in the source produce shadows of cyclic versions of the basic aperture pattern upon the detector, which need be only r by s in size.



GEOMETRY No.2

Fig. 4. This coded aperture arrangement employs only the basic r by s pattern for the aperture and has the disadvantage that the detector must be large enough to contain the image from the full field of view.



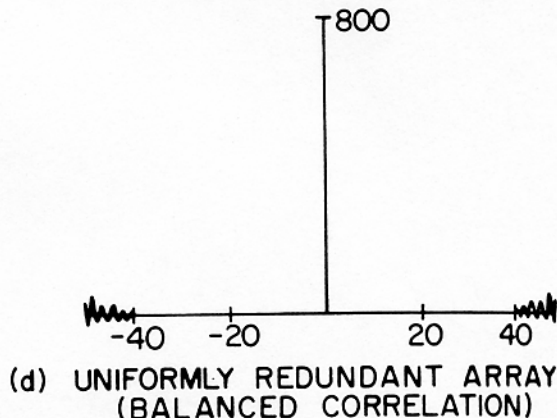
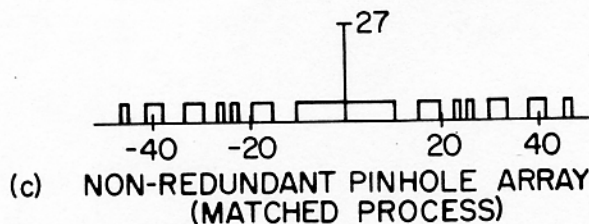
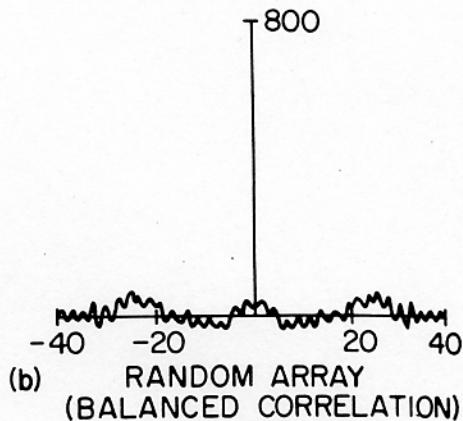
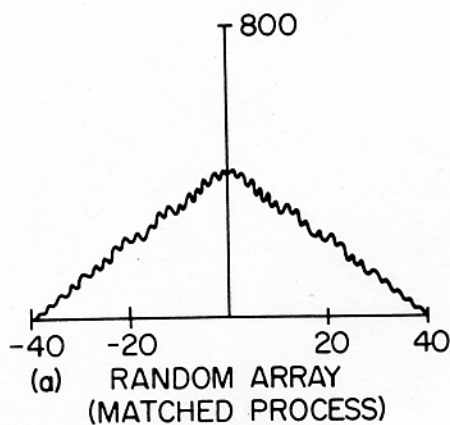


Fig. 6. (a) The system point-spread function (SPSF) for the random pinhole aperture and the matched decoding procedure. This and Fig. 6(b) represent the same 40×40 aperture. (b) The SPSF for the random pinhole aperture and the balanced correlation decoding procedure. The sidelobes have an expected value of zero, although some trends are possible. (c) The SPSF for the nonredundant pinhole aperture used in conjunction with the matched decoding procedure. Note the difference in the vertical scale from the accompanying graphs. The height of the small plateaus is 1. (d) The SPSF of the uniformly redundant array in conjunction with balanced correlation. Note that the sidelobes are deterministically zero out to ± 41 .

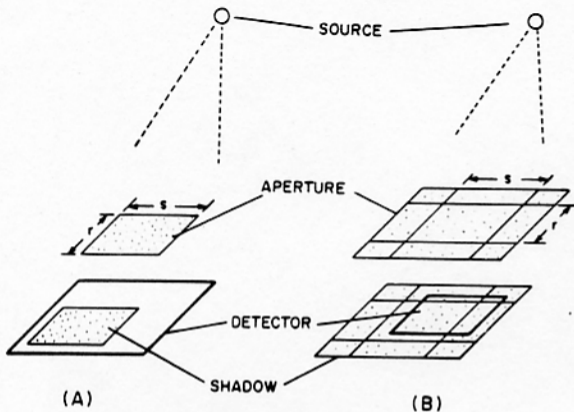


Fig. 1. (A) This coded aperture arrangement employs only the basic r by s pattern for the aperture and has the disadvantage that the detector must be large enough to contain the image from the full field of view. (B) This arrangement employs a $2r$ by $2s$ aperture composed of a mosaic of basic r by s patterns. Emitting points in the source produce shadows of cyclic permutations of the basic aperture pattern, and thus the detector needs to be only r by s in size.

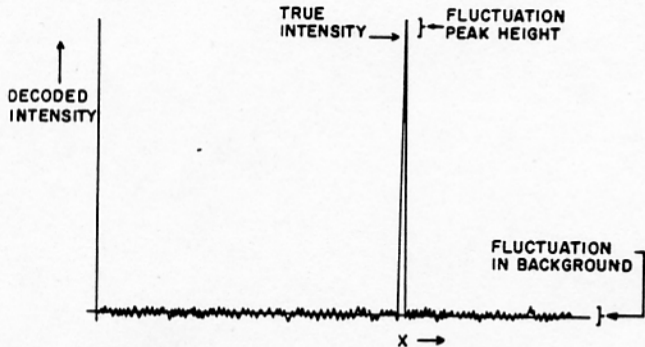


Fig. 2. A 1-D slice through a reconstructed object for a point source. The SNR is defined to be the peak height divided by the expected size of the fluctuations of the peak and the background.

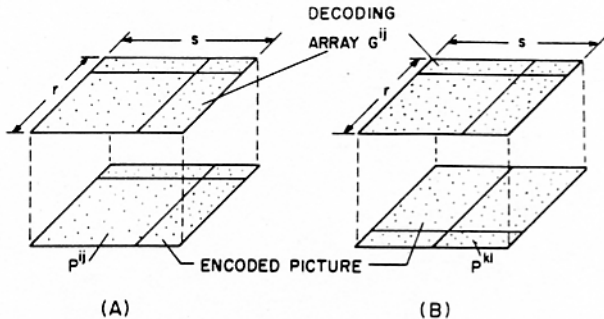


Fig. 3. (A) Orientation of the G array and the picture from the S_{ij} source when calculating the \hat{S}_{ij} point in the reconstructed object. (B) Same as A except the picture is due to the S_{kl} source.

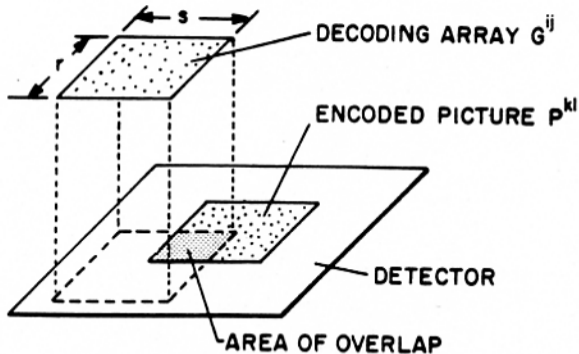


Fig. 4. Orientation of the G array and the picture from the S_{kl} source when calculating the \hat{S}_{ij} point in the reconstructed object. The random array geometry of Fig. 1(A) is assumed.

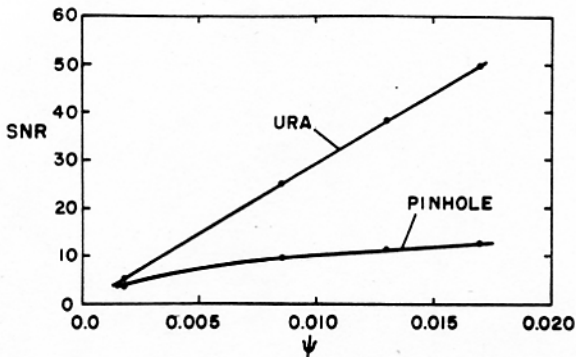


Fig. 6. Predicted SNR of a URA system and a pinhole camera for a source described in the text. Note that the improvement for the brighter points in the source (ψ large) is much better than for the low-intensity points.